DYNAMIC IMPACT RESPONSE OF NANOSIZED PRECIPITATES BEARING WASPALOY

Harrison Okechukwu Onovo*, David Ehigie Esezobor, and Muideen Adebayo Bodude
Department of Metallurgical and Materials Engineering, University of Lagos, Nigeria.

ABSTRACT: Dynamic response of nanosized precipitates bearing (NPB) Waspaloy, a class of superalloy, is crucial to design structural components for critical rotating applications and other severe dynamic impact predisposed applications. The focus of this study is, therefore, to investigate the compressive dynamic behaviour of NPB Waspaloy at a high strain rate under various deformation conditions. The technique of modified split Hopkinson pressure (MSHP) bar was implemented through impact deformation of Waspaloy under wide-ranging deformation temperatures (-180 - 750 ^{o}C) and strain rates of ($4*10^{3}$ - $7.5*10^{3}$ s^{-1}). The outcomes of the experiments divulge how to flow stress relates directly to strain rate and is inversely proportional to deformation temperatures. Work hardening rate affects NPB Waspaloy maximally at the iciest deformation temperature (-180 ^{o}C) and the highest strain rate ($7.5*10^{3}$ s^{-1}) considered. Under high straining and high rate of straining deformation conditions, the rate with which work-hardening occurs is destabilized due to the thermal softening effect during deformation. It is established that when strain is constant, the flow stress dependency on the rate of straining depicts linear relation. The thermal softening effect on NPB Waspaloy is concerted at around extreme strain rate ($7.5*10^{3}$ s^{-1}) and iciest deformation temperatures within -180 ~ 25 ^{o}C. Mapping of strain, strain rate and deformation temperatures representing input parameters with the resultant flow stress provide an unambiguous analytical view of the effects of dynamic impact deformation. Flow stresses at elevated temperatures are correlated directly with grain growth, mainly influenced by adopted deformation temperatures.

Keywords: Deformation, Stress-strain, Superalloy, Strain rate, Turbines, Mapping.

استجابة التأثير الديناميكي للمترسبات النانومترية في سبيكة الواسبالوي

هاريسون أ. أونوفو وديفيد إ. إيسيزوبور وميدين أ. بودود

الملخص: الاستجابة الديناميكية للمترسبات النانومترية المحملة في سبيكة الواسبالوي - وهي فئة من السبائك الفائقة - أمر بالغ الأهمية لتصميم المكونات الهيكلية للتطبيقات الدوارة الحرجة وغيرها من التطبيقات المعرضة للتأثيرات الديناميكية الشديدة. تركز هذه الدراسة، بالتالي، على استكشاف سلوك الضغط الديناميكي لسبيكة الواسبالوي المحملة بمترسبات نانومترية تحت معدلات تشوه عالية وظروف تشوه متنوعة. تم تنفيذ تقنية القضيب الضاغط المعدلة من هوبكنسون المقسم عبر تشوه التأثير للواسبالوي تحت درجات حرارة تشوه شاسعة (من -180 إلى 750 درجة مئوية) ومعدلات تشوه (من 4×10^{3} إلى 7.5×10^{3} ثانية$^{-1}$). تكشف نتائج التجارب كيف يرتبط إجهاد التدفق مباشرة بمعدل التشوه ويتناسب عكسيًا مع درجات الحرارة التشوهية. يؤثر معدل تقسية العمل في سبيكة الواسبالوي المحملة بمترسبات النانومترية بشكل أقصى عند درجة حرارة التشوه الأبرد (-180 درجة مئوية) وأعلى معدل تشوه معتبر (7.5×10^{3} ثانية$^{-1}$). تحت ظروف التشوه العالية ومعدل التشوه العالي، يتم تقويض معدل حدوث التقسية بسبب تأثير التراجع الحراري أثناء التشوه. يتم تأسيس أنه عندما يكون التشوه ثابتًا، فإن تبعية إجهاد التدفق على معدل التشوه تظهر علاقة خطية. يتركز تأثير التراجع الحراري على سبيكة الواسبالوي المحملة بمترسبات النانومترية عند معدل تشوه شديد (7.5×10^{3} ثانية$^{-1}$) ودرجات حرارة التشوه الأكثر برودة ضمن -180 ~ 25 درجة مئوية. توفر رسم الخرائط للتشوه ومعدله ودرجات حرارته كمعلمات إدخال مع إجهاد التدفق الناتج عرضًا تحليليًا واضحًا لآثار التشوه الناتج عن التأثير الديناميكي. يرتبط إجهاد التدفق عند درجات حرارة مرتفعة مباشرة بنمو الحبوب، والذي يتأثر بشكل رئيسي بدرجات الحرارة التشوهية المعتمدة.

الكلمات المفتاحية: تشوه؛ الإجهاد-التشوه؛ سبيكة فائقة؛ معدل التشوه؛ توربينات؛ رسم الخرائط.

Corresponding author's e-mail: honovo@unilag.edu.ng

DOI:10.53540/tjer.vol19iss2pp180-189

NOMENCLATURE

DHPB	Direct Hopkins pressure bar
SHPB	Split Hopkins pressure bar
MSHPB	Modified split Hopkins pressure bar
NPB	Nano precipitate bearing
FCC	Face-centred cubic crystal
EDM	Electric discharge machine
LOM	Light optical microscope
SEM	Scanning electron microscope
TEM	Transmission electron microscope

1. INTRODUCTION

Crucial materials applications susceptible to high-impact deformations necessitate the adoption of high-performance materials that can withstand impact deformations at high loading rates and avert components failure and/or catastrophic breakdown of materials while in service. The choice of such materials will not elude superalloys synonymous with good mechanical properties at elevated temperatures, which include retained high strength, outstanding corrosion resistance, good oxidation resistance together with the amazing blend of formability and toughness (Pollock and Sammy 2006, Liu *et al*. 2005). Superalloy Waspaloy essentially contains above 18% Chromium next to the base metal, Nickel, and is basically strengthened by precipitation hardening processes. The hardening procedure involves about three staggered heat treatment sequences, which commence with solution treatment, stabilizing by reheating, followed by age hardening treatments (Xue, 2018).

Waspaloy is a speciality alloy extensively used in critical applications like turbine combustion components and critical mechanisms of nuclear reactors, to mention a few, that are prone to dynamic impact deformations. Mostly, such applications require strength retentive materials with an additional high strength-to-weight ratio. Waspaloy's strength-to-weight ratio can be enhanced through the introduction of nanotechnology by tailoring the precipitation hardening phases to the nanoscale by means of controlled heat treatment (Veerappan *et al*. 2018).

Consequently, adequate knowledge and documentation of nano-scaled precipitation hardened Waspaloy high strain rates dynamic impacts response is indispensable to design structural components of Waspaloy for critical rotating applications and other severe dynamic impact predisposed applications. Well established and modified technique to study dynamic impact deformation (rate of material straining) of materials is the direct Hopkins Pressure Bar (DHPB) (Hopkinson, 1914), later altered to Split Hopkins Pressure Bar (SHPB) by Kolsky, as well known as Kolsky bar (Kolsky, 1949), and later improved to the modified Split Hopkins Pressure Bar (MSHPB) (Granier and Grunenwald, 2006), to uncover behavioural characteristics of materials subjected to high strain rate in the form of either compressive, tensile or torsional mechanical loading.

The role of materials' rate of straining in understanding materials' behaviour under dynamic impact loadings is very significant. Some pieces of literature have reported strain rates of soft and hard materials, which fall into either low or high loading rates. Materials strain rate sensitivity has been observed to increase precipitously beyond the critical region in a strain rate of about 1000 s^{-1} (Lee and Sun, 2004).

More so, the flow stress, generally and predominantly in metals with FCC, has been experientially reported to intensify progressively with a rising strain rate in areas beneath crucial points (Veerappan *et al*., 2018, Lee and Sun, 2004). Flow stress subsequently increases more swiftly as the deformation rate progresses beyond the critical region of the strain rate. Interestingly, the changeover of flow stress around the critical region has been ascribed to frequent alteration in the motion of dislocation (Regazzoni *et al*. 1987). Another school of thought opined that the transition could be regarded as enhanced rates of defeats formation, such as twin and dislocation.

Attention has been drawn to the reactional mirror of the flow stress-strain relation, which reveals the condition of innumerable microstructural arrangements throughout the deformation progression (Lee and Sun, 2004). As deformation progresses, the domineering stimulus of plastic behaviour of materials undergoing high impact (high strain rate) deformations are fundamentally the slip (dislocation) and twining defective mechanisms. Basically, the initial stage of the twinning mechanism requires a larger amount of stress as compared to the implementation of a dislocation slip. In addition, the multiplication of dislocation slip takes place very quickly at high strain rates deformations, from which the materials strengthening effect evolves (Lee *et al*. 2000, Gilbert *et al*. 2006). However, both twinning defects, as well as multiplicative dislocation improve the flow properties of metals, especially the strength (Li *et al*. 2010).

Scholarly investigations have reported some characteristic properties of Waspaloy. Investigations have documented the effects of aluminium and titanium content, together with the consequence of solution treatments, including microstructure, strength, and hardness (Chang and Liu 2001). The hot ductility has been studied (Andersson *et al*. 2013), as well as its tensile strength and creep behaviour (Wilshire and Scharning 2008), while the density has been estimated to be high, more than 95 % dense (Kamran *et al*. 2008). Further studies on Waspaloy focused on cyclic fatigue loading (Yeom *et al*. 2002), hardness and grain size (Stefan et al. 2010), the effect of gamma prime (Pike, 2008), and the electrical and mechanical properties (Whelchel *et al*. 2009).

Nevertheless, there is a paucity of experiential research reports on the dynamic impact behaviour of Waspaloy at extreme deformation conditions. The need to characterize high loadings dynamic impact response

and flow behaviour of Waspaloy is sensible and implementable through the modified compressive split Hopkinson pressure bar technique, which aids in establishing the correlation between the flow properties and the resultant microstructures of Waspaloy.

The present study, therefore, implements the latter technique to unfold comprehensive dynamic impact deformation and microstructural characteristics of Waspaloy at low and elevated temperatures for everyday service applications. This would put forward a wholistic investigational report of scarce Waspaloy's dynamic impact response at high strain rate deformation.

2. EXPERIMENTAL DESIGN

2.1. Materials Preparation

The major elemental composition of Waspaloy used in this study includes chromium, cobalt, molybdenum, titanium, iron, aluminium, and carbon, in mass per cent (%) as 19.5, 13.5, 4.3, 3, 2, 1.4, and 0.07, respectively, and was sourced in plate form from Prof. AO Ojo of the Mechanical Engineering Department, University of Manitoba, Canada. The cylindrical specimens' dimension in mm is 9.5 by 10.5 (diameter by height) and were smoothly sectioned out with an electric discharge machine (EDM) (Asala *et al*. 2019).

2.2. Development of NPB Waspaloy

Prior to dynamic impact testing, specimens were developed into NPB particles through lengthy thermal treatment processes and controlled cooling rate, as illustrated in Fig. 1. The key hardening features of waspaloy are the precipitated gamma prime particles, which has its sizes beyond nanoscale in normal wrought condition. The three major conditions that encourage the formation of particles in waspaloy are temperature, soaking period and cooling rate.

Customarily, exceptional properties of metallic alloys are achieved at the nanoscale, and to tailor NPB waspaloy, lengthy thermal treatments (solution treatment, stabilization and age-harden), different soaking time, and various thermal cooling processes ranging from 0.25 - 500 ^{o}C/s was implemented. However, it was found that a cooling rate of 28 - 30 ^{o}C/s effectively yielded the envisaged NPB Waspaloy. This implies that any deviation in the aforementioned procedures and conditions will set undesirable results in motion.

The surfaces of the specimens were smoothened by polishing them with emery paper of 1600 grits in order to accomplish NPB waspaloy, while Al_2O_3 liquid (0.6 µm particle size) was used to buff-polished the surfaces to minimize shear and frictional forces during impact deformation. Molybdenum disulfide grease was used at the ends of the specimen to lubricate its surfaces and hence reduce effects from frictional forces.

Post-surface smoothening is the specimen particle size range estimation and resolution during synthesis,

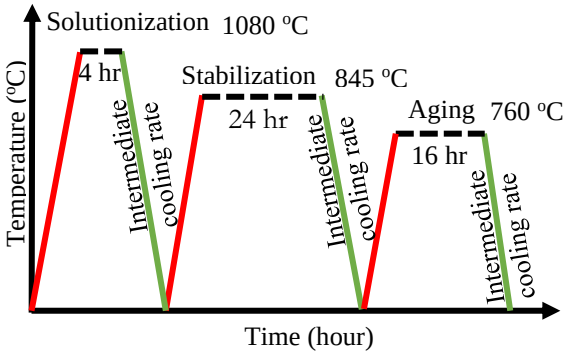

Figure 1. Thermal treatment conditions and cooling processes adopted for synthesis of NPB Waspaloy.

which proved difficult with a light optical microscope (LOM) together with the scanning electron microscope (SEM), as the resulting images were imperceptible. Hence, a high-resolution transmission electron microscope (TEM) aids in resolving the synthesized nanoparticle sizes. The nanoparticle structure was inspected with the JEOL 2010F transmission electron microscope domesticated at the University of Manitoba.

The microscope has an auxiliary EDAX ultrathin window detector. The TEM samples were ground to thin foils and polished using emery paper from 800 to 1500 grits to about 100 µm thick. Coupons 3 mm in diameter were then punched out from the polished thin foils, followed by dimpling and electropolishing processes. Twin-jet electro-polisher was adopted for coupons electropolishing in a solution containing alcohol of 90 % methyl and acid of 10% perchloric at the following approximate conditions: temperature (-40 ^{o}C), voltage (1.5 V) and current (1.5 DC) (Asala *et al*. 2016).

2.3. High strain rate deformation of NPB Waspaloy

High-strained impact tests were conducted at high strain laboratory, Mechanical Engineering, University of Manitoba, using a compressive SHPB at wide-ranging high strain rates varied from $4*10^3$ - $7.5*10^3$ s^{-1} with deformation temperatures between -180 ^{o}C to 750 ^{o}C.

3. RESULTS AND DISCUSSION

3.1. Evolution of Flow Stress

Dynamic impact response of NPB waspaloy deformed under wide-ranging strain rates: $4*10^3$ to $7.5*10^3$ (s^{-1}) at diverse deformation temperatures from -180 to 750 ^{o}C are presented in Figs. 2a through d.

The mechanical and flow behaviour of the deformed specimens is, to a large extent, reliant on the deformation parameters such as the rate of straining and temperature of NPB Waspaloy specimens. The flow stress rapidly upsurges from the inception of dynamic deformation or low strains for each dynamic loading condition. It increases sluggishly at larger strains.

The observed surge in flow stress from the onset of

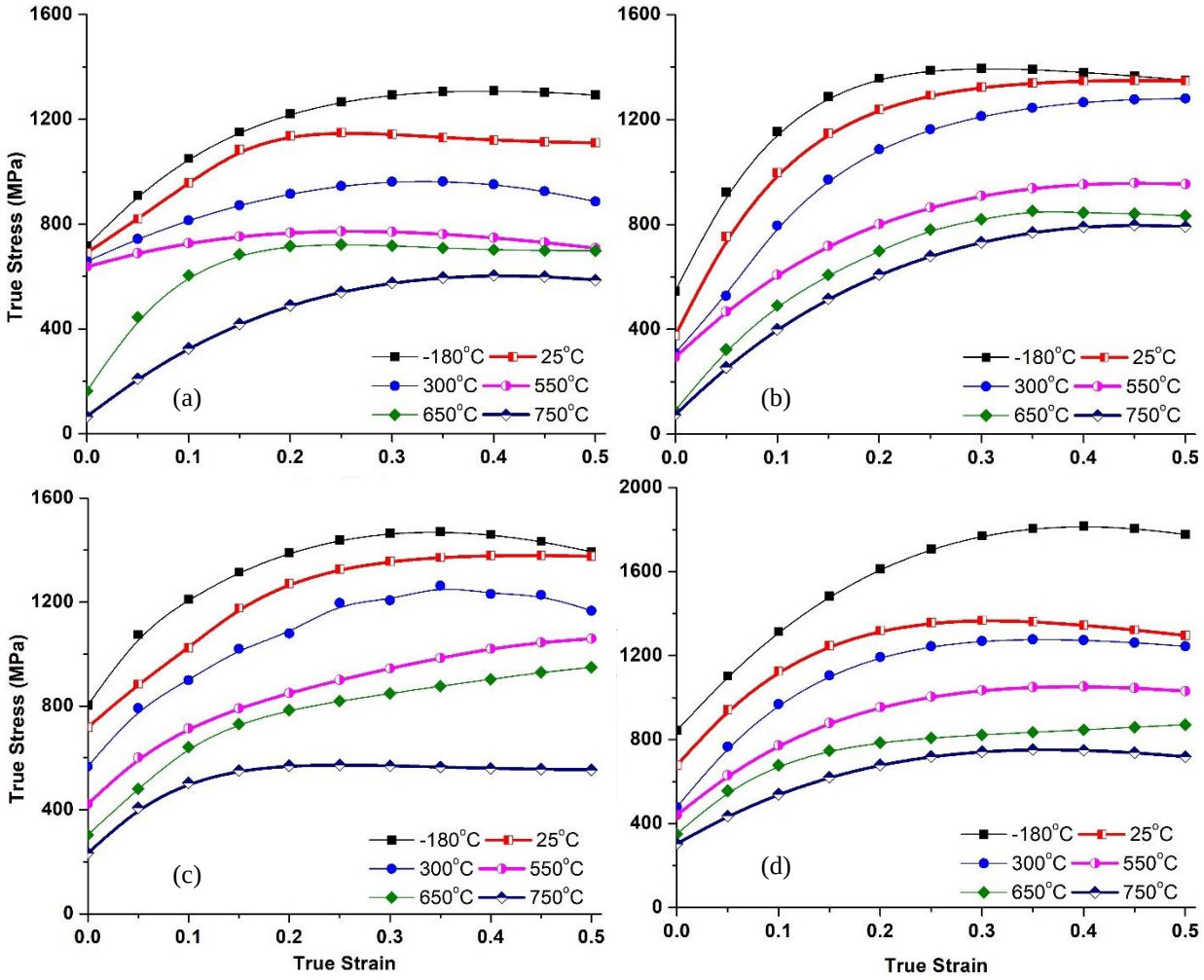

Figure 2. Comparison of dynamic impact response of NPB Waspaloy as flow stress at constant strain rate: (a) $4*10^3$ s^{-1}, (b) $5*10^3$ s^{-1}, (c) $6*10^3$ s^{-1}, (d) $7.5*10^3$ s^{-1} under varied deformation temperatures (-180 – 750 °C).

impact deformation could be linked to the formation and intensification of dislocation density together with the growth of sub-grain boundaries, which emanate from dynamic recovery and working hardening of materials (Wang *et al*. 2008). Beyond the peak stress region, flow stress declines as strain rises in magnitude. Flow stress declination occurs when the strain rate hardening effect, in addition to strain, prevails through the thermal softening effect introduced by heat generated during dynamic impact deformation of materials (Chiou *et al*. 2009). Fig. 2(a to d) shows noticeable flow stress declination as the strain rate remains steady and the deformation temperature rises. Besides, under constant deformation temperature, strain rates energies rise changes in flow stress, which rises, which rises significantly as the strain rate also rises from $4*10^3$ to $7.5*10^3$ (s^{-1}) on the impacted NPB Waspaloy. These results are in good trend with earlier statements (Srinivasan *et al*. 1993, Garcia *et al*. 1994, Lee and Sun 2004, Zhou and Baker 1994, Lee *et al*. 2005, Yuan and Liu 2005, Thomas *et al*. 2006, Wang *et al*. 2008, Lee *et al*. 2011, Lee and Kao 2014) that reported the relation of high dynamic impact deformations to different loading conditions of other superalloys.

3.2. 3D Mapping of Dynamic Impact Response of NPB Waspaloy

Nascent innovative techniques will not elude the implementation of data mapping for unabridged descriptive analysis of the continuous relationship of deformation parameters which include strain rate and deformation temperature. Earliest in data mapping of deformation behaviour considered contourable 2D data mapping of deformation parameters focusing on strain rate and deformation temperature, which confirms that strain rate sensitivity parameter varies directly with deformation temperature but inversely to strain rate (Garcia *et al*. 1994). Additionally, the first attempt at 3D mapping is a rhombus data matrix conducted at a steady strain rate for deformation temperature, strain and stress (Quan *et al*., 2013). This data mapping is faulted (Quan *et al*. 2016), as stress is analyzed as an input effect of deformation rather than a resultant expressive effect. Further, the first apt 3D data mapping was applied to ensuing stress data with varied temperatures, strain rate and strain (Quan *et al*. 2016). This study, however, implements the most suitable 3D

mapping of experiential data of Waspaloy dynamically deformed to further investigate the unceasing relationship existing among deformation parameters of temperature, flow stress, strain rate, and strain.

Dissimilar to stress ~ strain relation in 2D, the maps of experiential response data in 3D are demonstrated by diverse colour shades. The 3D data mapping is unceasing and avails the choice of interpreting response data (flow stress) as a block of data (Figure 3a) in three fundamental orientations (x-, y-, and z-axis). It is also applicable to any constant deformation parameters that include strain, deformation temperature, and strain rate,

as presented in Figure 3b. Figure 3c presents the deformation behaviour of Waspaloy at constant strain but varied deformation temperature together with strain rate, which further validates the region of ultimate flow stress to fall between the strain value of 0.3 and 0.4.

Similarly, Figure 3d represents the deformation characteristics of Waspaloy at a fixed strain rate, which obviously reveals that flow stress progresses as the strain rate increases. Likewise, at fixed deformation temperature, Figure 3e shows that flow stress is maximum at the iciest temperature, denoting a decline

in flow stress as deformation temperature upsurges, while Figure f attempts to expose the inner portions of the mapped data by showing the flow stress distributions at the initial and middle points of each of the deformation parameters under scrutiny. Evidently, the deformation response at different conditions considered is more visually appreciated in comparison to the conventional 2D stress ~ strain relation.

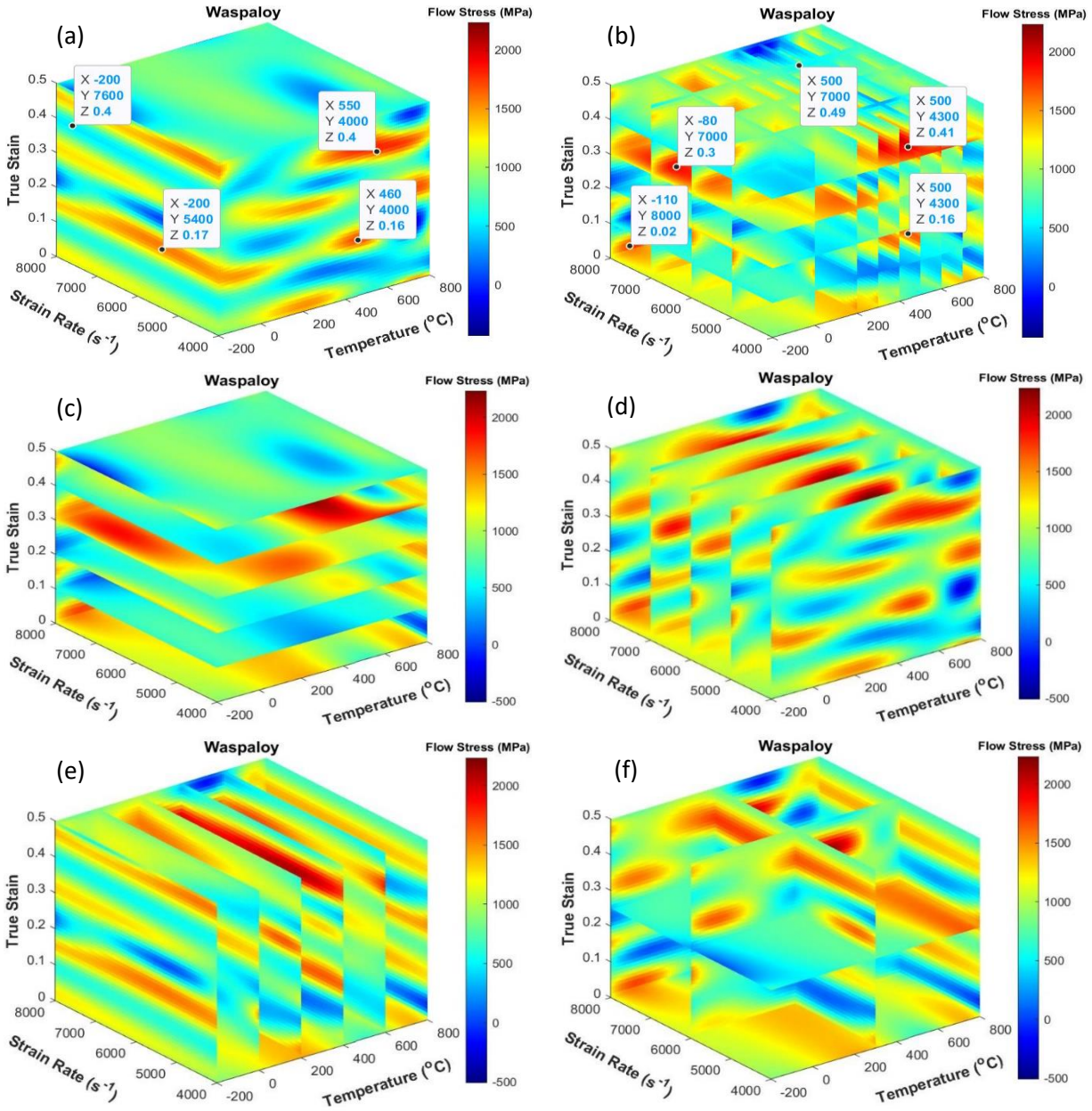

Figure 3. 3D map of NPB Waspaloy flow stress distribution at constant (a) no constant parameter (block), (b) strain rate, strain and deformation temperature, (c) strain, (d) strain rate, (e) deformation temperature, and (f) initial and middle point of each deformation parameter.

From the foregoing, the interpolative and extrapolative practicability of 3D mappings are not exhaustive yet and cannot be exaggerated as the resultant data for any deformation condition (deformation temperature, strain rate and strain) could be domiciled in the research database to enable and enhance analysis on impact deformation response of Waspaloy. The enriched populated data can be converted via different programming languages into finite element modelling (FEM) accepted formats and introduced into FEM for further simulative analytical approach in different areas of study and hence, curb the rigorous and expensive investigational processes.

3.3. Flow stress reliance on strain rate

Reliance of flow stress on strain rate at the specific strain, in addition to deformation temperatures, is portrayed in Figures 4(a, b and c) and 5(a, b and c), which further illustrate the existing relationship amid Waspaloy's deformation parameters: deformation temperature, and strain rate sensitivity. Evidently, a steady strain rate and strain, increasing the deformation temperature, suggest an attendant decrease in flow stress. Invariably, flow stress increases under steady strain and deformation temperature as the strain rate increases, which confirms Waspaloy's strain rate sensitivity. From Figures 4 and 5, the flow stress at a fixed temperature (-180 ^{o}C) and strain rate ($4*10^3$ s^{-1}) increased from 1051 to 1221 to 1613 MPa. This corresponds to plastic strains: 0.1, 0.2 and 0.3, respectively. Flow stress increase is observed to be consistent as seen across other corresponding deformation temperatures with regard to strain rates under various compressive impact deformation conditions considered. Flow stress resulting from strain rate of ($4*10^3$ s^{-1}) and strain (0.1) (Figure 4) increased from 326 to 1051 MPa as deformation temperature decreased from 750 to -180 ^{o}C, respectively. The behaviour is evident in another strain rate ($5*10^3$ to $7.5*10^3$ s^{-1}) and strain 0.2 to 0.3 under discourse. Consequently, NPB Waspaloy exposed to high dynamic impact deformation depends to a large extent on the deformation temperature.

3.4. Effect of Thermal Softening

The specimen's property, such as thermal conductivity and the rate at which the material is deformed, accounts for the different influences apparent on the plastic behaviour, which is attributed to the adiabatic softening effect on materials. Incidentally, the heat generated during low strain rates deformation typically has sufficient time to dissipate or escape into the environment as deformation progresses, thereby causing little or no effect on the specimen's temperature being tested, resulting in isothermal deformation testing. However, high strain rate deformation occurs so fast (within a split second) that there is no ample time for the heat generated during deformation to disperse away, and this paves the way for heat accumulation within the specimen, which invariably affects the behavioural dispositions of the specimen undergoing dynamic impact deformation. The phenomenal testing situation is fundamentally denoted as an adiabatic heating condition. Strikingly, the resultant effect of adiabatic heating conditions grossly influences the thermal softening of materials (Shi *et al.* 2014). Essentially, the effect of a swift rise in temperature during plastic deformation is generally expressed by Equation (1):

$$\Delta T = \frac{\beta}{\rho * C_p} \int_0^{\varepsilon} \sigma * d\varepsilon \qquad (1)$$

where $\Delta T, \varepsilon, C_p, \rho, and\ \sigma$ are the temperature rise in Waspaloy while undergoing plastic deformation, true axial stress, the axial plastic strain, density (g/cm^3), and specific heat (J/g.K) respectively. Density, ρ is taken to be 8.19 (g/cm^3), heat capacity C_p is 435 (J/g.K), stress σ is the flow stress and strain interval $d\varepsilon$, which corresponds to true strain.

As the integral function in Equation (1) denotes the total plastic work done on the specimen, β is a fractional representation of total work from plastic deformation, transformed into heat, with a conventional value of 0.9. The thermal softening effect accounts for the reduction or outright loss of the material's strain or work-hardening capabilities (Ranc and Chrysochoos, 2013). Figures 6(a to d) show the disparity of the rise in temperature during deformation regarding the true strain at fixed deformation temperatures and strain rate. Temperature rise, ΔT and true strain increase proportionately at a constant strain rate. However, with temperature rise, ΔT has a reverse trend with respect to deformation temperature. In all the loading conditions for direct impact deformation Waspaloy in discourse, the maximum thermal softening or temperature rise effect takes place at the iciest temperature (-180 ^{o}C) and maximum strain rate ($7.5*10^3$ s^{-1}) in the impacted specimen.

3.5. Rate of Work-Hardening

Flow stress-strain graphs at various impact deformation conditions (Figure 2a to d) demonstrate work hardening tendencies. Figures (12 to 15) provide the disparity of the work-hardening rate $\left(\partial\sigma/_{\partial\varepsilon}\right)$ with respect to different deformation temperatures from -180 to 750 (^{o}C) and true strains from 0.1 to 0.5 as well as various strain rates from $4*10^3$ to $7.5*10^3$ (s^{-1}). Thus, the rate at which work-hardening occurs is subject to prime agents of plastic deformation mechanisms, which include strain, deformation temperature, and strain (loading) rate. Manifestly, the maximum work-hardening effects recorded in this study occur at the iciest deformation temperature (-180 ^{o}C), the primary stage of true strain (approximately 0.2) and the maximum strain rate ($7.5*10^3$ s^{-1}). The work-hardening rate of Waspaloy reduces simultaneously as strain and deformation temperatures rise, as contained in Figure 7 (a to d). Deformation temperature rise in compressive high

strain rate deformation is attributable to adiabatic heating, which occurs when the impact energy utilized in deforming metallic materials is wholly transformed into heat energy, but then, the heat energy generated is somewhat lockup in the metal, as it is not swiftly dissipated to the metal's surroundings, thereby increasing the overall temperature level of the metal.

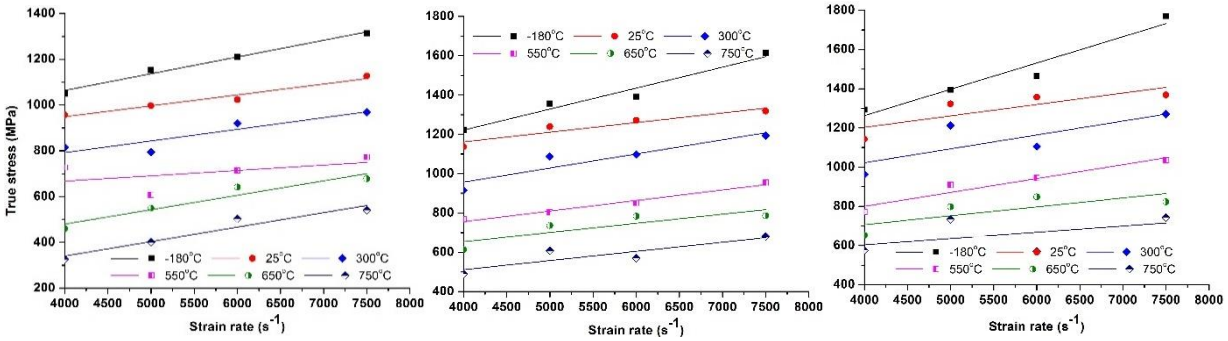

Figure 4. Dependency of flow stress on strain rate at fixed deformation temperature and varied strain: (a) 0.1, (b) 0.2 and (c) 0.3.

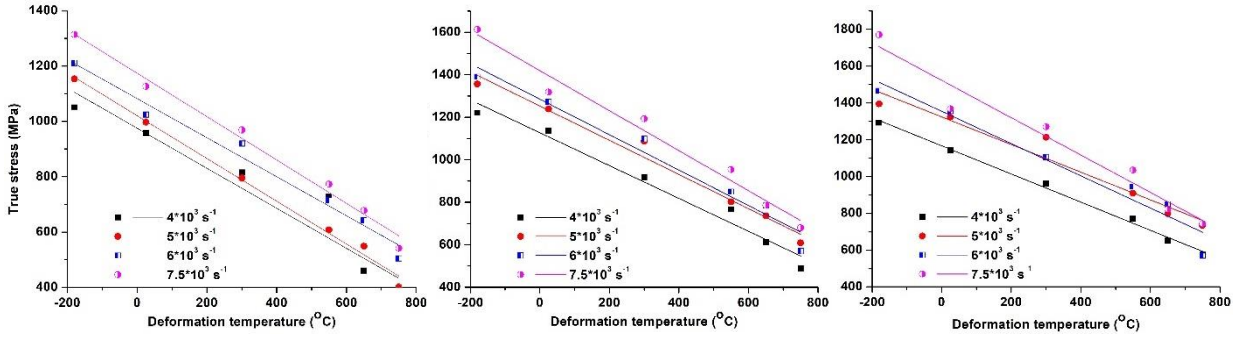

Figure 5. Dependency of flow stress on deformation temperature at fixed strain rate and varied strain: (a) 0.1, (b) 0.2 and (c) 0.3.

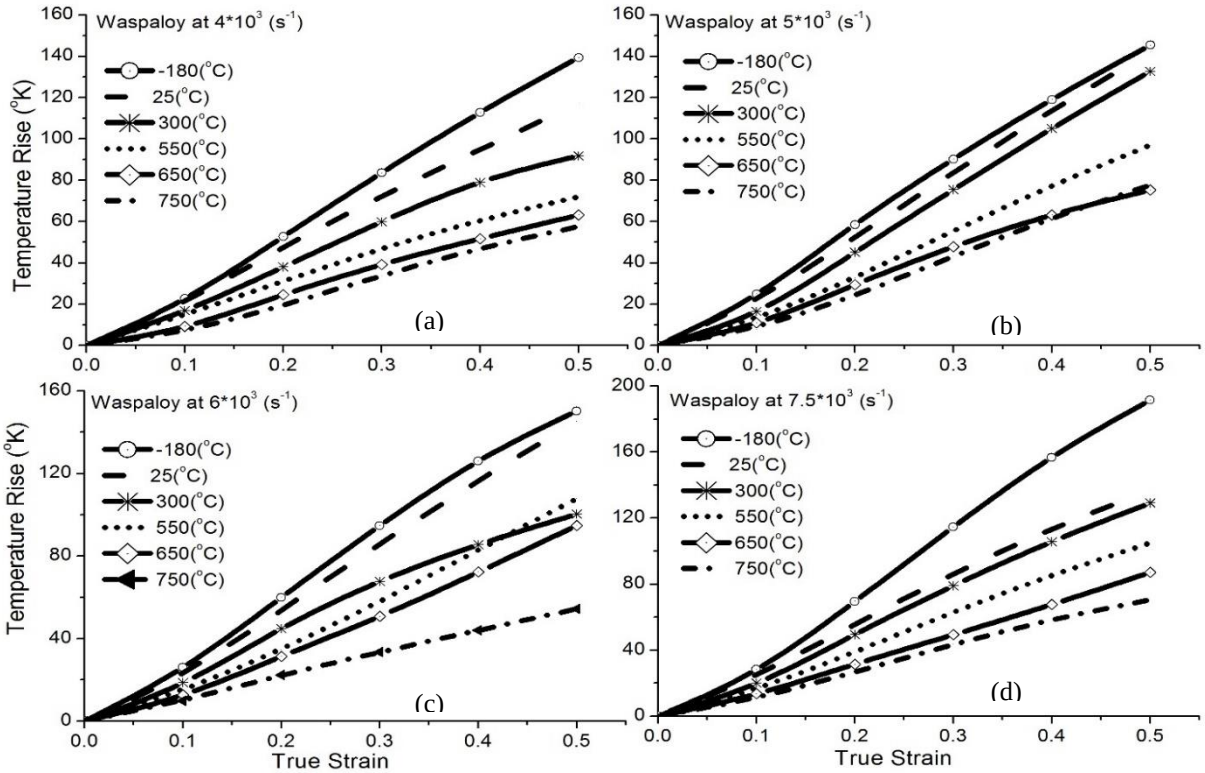

Figure 6. Temperature rise, ΔT during plastic deformation of NPB waspaloy at constant strain, varied strain rate: (a) $4*10^3$ s^{-1}, (b) $5*10^3$ s^{-1}, (c) $6*10^3$ s^{-1}, (d) $7.5*10^3$ s^{-1} and different temperature (-180 – 750 °C).

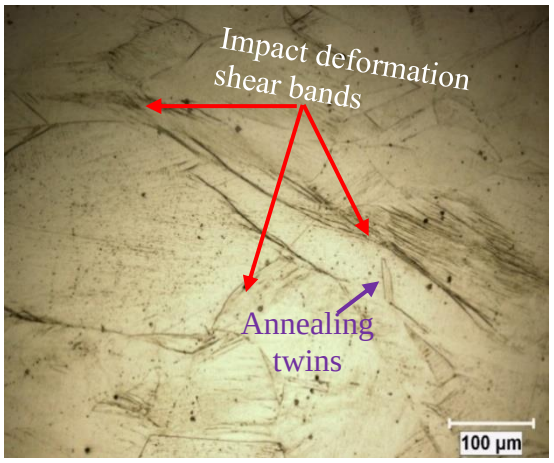

Plate 1. Light optical image of Waspaloy impacted at $\dot{\varepsilon}\ 6 * 10^3$ (s^{-1}) and 25 (^oC).

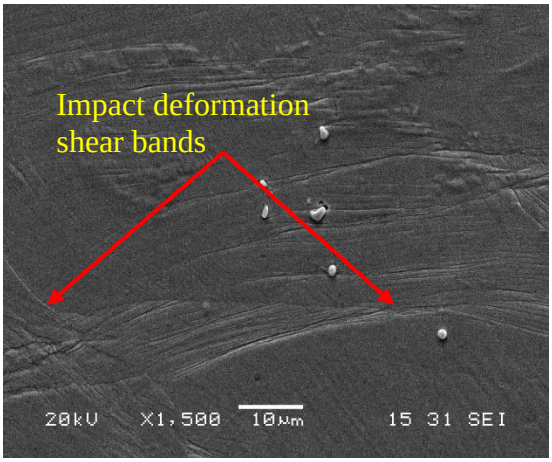

Plate 2. Scanning electron image of Waspaloy impacted at $\dot{\varepsilon}\ 6 * 10^3$ (s^{-1}) and 25 (^oC).

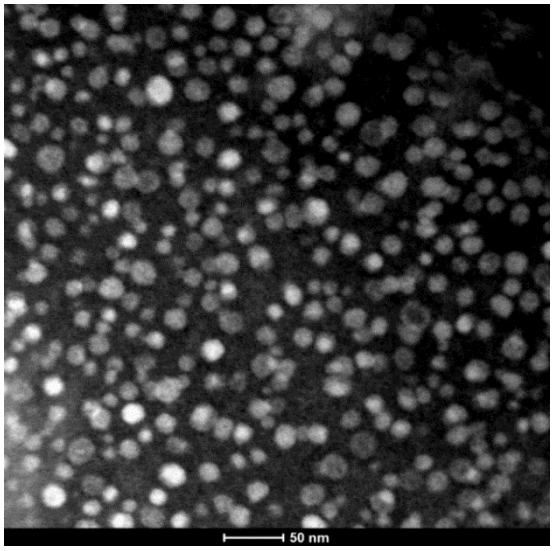

Plate 3. TEM images of NPB particles Waspaloy.

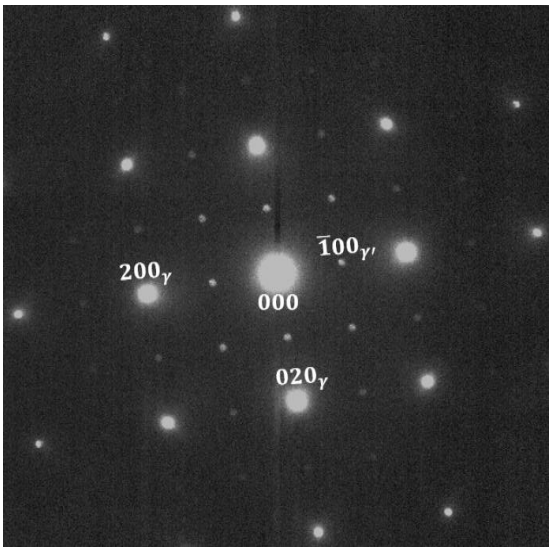

Plate 4. TEM images of NPB Waspaloy with SADP indexing.

Conversely, for fixed deformation temperature, and strain, the work-hardening rate perpetually rises concurrently with the strain rate. Hence, the thermal softening consequence is a resultant outcome of a rise in temperature during dynamic impact deformation. Convincingly, the rate with which work hardening of Waspaloy occurs, demonstrates consistent positive effects for every value of true strain (0.1 to 0.5), strain rate ($4*10^3$ to $7.5*10^3$ s^{-1}) and deformation temperature (-180 to 750 ^oC). However, the dynamic work hardening effect is established to dominate thermal softening results on Waspaloy specimens studied under stable dynamic plastic deformation at dissimilar conditions: deformation temperatures (low and high) and strain rate (high) loading situations (Lee *et al*. 2011).

3.6. Microstructural Examination

The light optical microscopy and scanning electron microscopy of dynamically impacted NPB Waspaloy at a high strain rate ($6*10^3$ s^{-1}), room (25 ^oC) temperature is singled out for reasons of conspicuous presence of deformation shear bands which exposed the occurrence of dense dislocation and straight annealing twins' (lamella-like) substructures (Plates 1 and 2). The annealing twins present depicts the viability of systematic changes in crystals as a result of cooling effects. Moreso, the shear bands being a softening mechanism, leads to an abrupt decrease in flow stress due to inhomogeneous plastic deformation. The During transmission electron microscopic (TEM) examination (Plate 3 and 4), the diffraction patterns were investigated, which reveal that the Waspaloy gamma prime diffraction pattern is on the 001 zone, while the micrographs disclose the range of particle sizes within the nanometer scale.

CONCLUSION

1. The cooling rate of 28-30 $^oC/s$ effectively

produced NPB Waspaloy.
2. Nanoscale precipitation hardened Waspaloy flow stress improvement at strain rate recommends its suitability for applications where high dynamic impact competence is a design consideration.
3. The declination of flow stress values at elevated temperatures is traceable to grain growth grossly encouraged by the deformation temperature.
4. Dynamic work hardening effect influences the outcome of thermal softening under stable dynamic plastic deformation

ACKNOWLEDGEMENTS

The superalloy samples, technical know-how, laboratories, reagents, equipment and pieces of machinery used in this study were provided by Professor Olanrewaju A. Ojo of the Mechanical Engineering Department, University of Manitoba, Canada. The authors are grateful to him and his research team.

REFERENCES

Andersson, J., Sjoberg, G. P., Viskari, L., & Chaturvedi, M. (2013). Effects of different solution heat treatments on the hot ductility of superalloys. *Journal of Materials Science and Technology*, 29, 43-53.

Asala, G., Andersson, J., & Ojo, O. A. (2016). Precipitation behavior of γ′ precipitates in the fusion zone of TIG welded ATI 718Plus®. International *Journal of Advanced Manufacturing Technology*, 87, 2721-2729.

Asala, G., Andersson, J., & Ojo, O. A. (2019). A study of the dynamic impact behaviour of IN 718 and ATI 718Plus® superalloys. Philosophical Magazine, 99(4), 419-437.

Chang, K-M., & Liu, X. (2001). The effect of γ′ content on the mechanical behaviour of the WASPALOY alloy system. *Journal of Materials Science and Engineering* A, 308, 1-8.

Chiou, S-T., Tsai, H-L., & Lee, W-S. (2009). Impact mechanical response and microstructural evolution of Ti alloy under various temperatures. *Journal of Materials Processing Technology*, 209(5), 2282-2294.

Gilbert, A., Wilcox, B. A., & Hahn, G. T. (2006). The effect of strain rate on dislocation multiplication in polycrystalline molybdenum. *The Philosophical Magazine: A Journal of Theoretical Experimental and Applied Physics*, 12(117), 649-653.

Granier, N., & Grunenwald, T. (2006). A modified split Hopkinson pressure bar for toughness tests. *Journal of Physics IV France*, 134, 813-818.

Hopkinson, B. (1914). A method of measuring the pressure produced in the detonation of high explosives or by the impact of bullets. Philosophical Transactions of the Royal Society of London. Series A, Containing Papers of a Mathematical or Physical Character, 213(437), 497-508.

Kamran, A. M., Poonjolai, E., & Neil, H. (2008). High-density selective laser melting of Waspaloy. *Journal of Materials Processing Technology*, 195(1-3), 77-87.

Kolsky, H. (1949). An investigation of the mechanical properties of materials at very high rates of loading. Proceedings of the Physical Society B, 62(11), 676-700.

Lee, W. S., Shyu, J. C., & Chiou, S. T. (2000). The effect of strain rate on impact response and dislocation substructure of 6061-T6 aluminium alloy. Scripta Materialia, 42(1), 51-56.

Lee, W-S., & Kao, H-C. (2014). Impact deformation and fracture behaviour of cobalt-based Haynes 188 superalloy. World Academy of Science, Engineering and Technology. *International Journal of Chemical, Molecular, Nuclear, Materials and Metallurgical Engineering*, 8(8), 774-778.

Lee, W-S., & Sun, T-N. (2004). Plastic flow behaviour of Inconel 690 super alloy under compressive impact loading. Materials Transactions, 45(7), 2339-2345.

Lee, W-S., & Sun, T-N. (2004). Plastic flow behaviour of Inconel 690 super alloy under compressive impact loading. Materials Transactions, 45(7), 2339-2345.

Lee, W-S., Lin, C-F., Chen, T-H., & Chen, H-W. (2011). Dynamic impact response of Inconel 718 alloy under low and high temperatures. Materials Transactions, 52(9), 1734-1740.

Lee, W-S., Liu, C-Y., & Sun, T-N. (2005). Dynamic impact response and microstructural evolution of Inconel 690 superalloy at elevated temperatures. *International Journal of Impact Engineering*, 32, 210-223.

Li, X., Wei, Y., Lu, L., Lu, K., & Gao, H. (2010). Dislocation nucleation governed softening and maximum strength in nano-twinned metals. Nature, 464, 877-880.

Liu, H-S., Yan, B-H., Huang, F-Y., & Qiu, K-H. (2005). A study on the characterization of high nickel alloy micro-holes using micro-EDM and their applications. *Journal of Materials Processing Technology*, 169, 418-426.

Pike, L. M. (2008). Development of a fabricable gamma-prime (γ') strengthened superalloy. TMS. https://www.tms.org/superalloys/10.7449/2008/Superalloys_2008_191_200.pdf.

Pollock, T. M., & Sammy, T. (2006). Nickel-based superalloys for advanced turbine engines: Chemistry, microstructure and properties. *Journal of Propulsion and Power*, 22, 361-374.

Quan, G-Z., Lv, W-Q., Mao, Y-P., Zhang, Y-W., & Zhou, J. (2013). Prediction of flow stress in a wide temperature range involving phase transformation for as-cast Ti–6Al–2Zr–1Mo–1V alloy by artificial neural network. Materials and Design, 50, 51-61.

Quan, G-Z., Zhang, Z-H., Zhou, Y., Wang, T., & Xia, Y-E. (2016). Numerical description of hot flow

behaviors at Ti-6Al-2Zr-1Mo-1V alloy by GA-SVR and relative applications. Materials Research, 19(6), 1-17.

Ranc, N., & Chrysochoos, A. (2013). Calorimetric consequences of thermal softening in Johnson-Cook's model. Mechanics of Materials, 65, 44-55.

Regazzoni, G., Kocks, U. F., & Follansbee, P. S. (1987). Dislocation kinetics at high strain rates. Acta Metallurgica, 35(12), 2865-2875.

Shi, C., Lai, J., & Chen, X. G. (2014). Microstructural evolution and dynamic softening mechanisms of Al-Zn-Mg-Cu alloy during hot compressive deformation. Materials, 7(1), 244-264.

Srinivasan, R., Ramnarayan, V., Deshpande, U., Jain, V., & Weiss, I. (1993). Computer simulation of the forging of fine grain IN-718 alloy. Metallurgical Transactions A, 24(9), 2061-2069.

Stefan, O., Anders, W., & Goran, S. (2010). The effect of grain size and hardness of Waspaloy on the wear of cemented carbide tools. *International Journal of Advanced Manufacturing Technology*, 50, 907-915.

Thomas, A., El-Wahabi, M., Cabrera, J. M., & Prado, J. (2006). High temperature deformation of Inconel 718. Materials Processing Technology, 177(1-3), 469-472.

Veerappan, G., Ravichandran, M., & Marichamy, S. (2018). Mechanical properties and machinability of waspaloy for aerospace applications – a review. IOP Conference Series: Materials Science and Engineering, 402, 012039.

Wang, Y., Shao, W. Z., Zhen, L., Yang, L., & Zhang, X. M. (2008). Flow behaviour and microstructures of superalloy 718 during high temperature deformation. Materials Science and Engineering A, 497, 479-486.

Whelchel, R. L., Kelekanjeri, V. S. K. G., & Gerhardt, R. A. (2009). Mechanical and electrical characterization in age-hardened Waspaloy microstructures. International Heat Treatment and Surface Engineering, 3(1-2), 35-39.

Wilshire, B., & Scharning, P. J. (2008). Theoretical and practical approaches to creep of Waspaloy. *Journal of Materials Science and Technology*, 25(2), 242-248.

Xue, L. (2018). Chapter 16 - Laser consolidation—A rapid manufacturing process for making net-shape functional components. In J. Lawrence (Ed.), Advances in Laser Materials Processing (pp. 461-505). Woodhead Publishing.

Yeom, J. T., Williams, S. J., & Park, N. K. (2002). Low-cycle fatigue life prediction for Waspaloy. *Journal of Materials at High Temperatures*, 19(3), 153-161.

Yuan, H., & Liu, W. C. (2005). Effect of the δ phase on the hot deformation behaviour of Inconel 718. Materials Science and Engineering A, 408(1-2), 281-289.

Zhou, L. X., & Baker, T. N. (1994). Effects of strain rate and temperature on deformation behaviour of IN 718 during high temperature deformation. Materials Science and Engineering A, 177(1-2), 1-9.